

Probing Adsorption Sites of Silica-Supported Platinum with $^{13}\text{C}^{16}\text{O} + ^{12}\text{C}^{16}\text{O}$ and $^{13}\text{C}^{18}\text{O} + ^{12}\text{C}^{16}\text{O}$ Mixtures: A Comparative Fourier Transform Infrared Investigation

Victor Y. Borovkov,[†] Stanislav P. Kolesnikov,[†] Vladimir I. Kovalchuk,[‡] and Julie L. d'Itri^{*,‡}

N. D. Zelinsky Institute of Organic Chemistry RAS, 117913 Moscow, Russia, and Department of Chemical Engineering, University of Pittsburgh, Pittsburgh, Pennsylvania 15261

Received: April 2, 2005; In Final Form: August 5, 2005

A comparative investigation of the adsorption of $^{13}\text{C}^{18}\text{O} + ^{12}\text{C}^{16}\text{O}$ and $^{13}\text{C}^{16}\text{O} + ^{12}\text{C}^{16}\text{O}$ mixtures on silica-supported Pt has been conducted. It is advantageous to use $^{13}\text{C}^{18}\text{O} + ^{12}\text{C}^{16}\text{O}$ mixtures rather than $^{13}\text{C}^{16}\text{O} + ^{12}\text{C}^{16}\text{O}$ to probe the adsorption sites and electronic state of supported Group VIII metals because the vibrational bands of the adsorbed $^{13}\text{C}^{18}\text{O}$ and $^{12}\text{C}^{16}\text{O}$ isotopic molecules do not overlap. In addition, while an intensity redistribution suppresses the lower-frequency band with adsorbed $^{13}\text{C}^{16}\text{O}$ and $^{12}\text{C}^{16}\text{O}$ with vibrational frequencies differing by 50 cm^{-1} , the intensity redistribution is less pronounced with the adsorbed $^{13}\text{C}^{18}\text{O}$ and $^{12}\text{C}^{16}\text{O}$ in which the frequency difference is 100 cm^{-1} . Moreover, the small intensity redistribution that does occur between the bands of adsorbed $^{13}\text{C}^{18}\text{O}$ and $^{12}\text{C}^{16}\text{O}$ still allows the detection of the vibrational band of adsorbed $^{13}\text{C}^{18}\text{O}$ at $^{13}\text{C}^{18}\text{O}$ gas-phase concentrations as low as 3%. At such low concentrations, the dipole–dipole interaction between adsorbed $^{13}\text{C}^{18}\text{O}$ molecules is negligible, and, hence, both the singleton frequency and the dipole–dipole shift for adsorbed CO may be obtained in a single experiment. Two types of strongly bound and one type of weakly bound linear CO–Pt adsorption complexes have been identified and characterized by their singleton frequencies and dipole–dipole coupling shifts. The origin of these CO adsorption modes is discussed.

Introduction

It is essential to have knowledge regarding the geometric and electronic properties of the active site in order to understand catalysis by transition metals. Often the information is inferred from the vibrational frequency of noninteracting CO molecules adsorbed in a linear mode and from the shift of the absorption band maximum that results from dipole–dipole interactions between adjacent CO molecules on the metal surface.^{1–3} The vibrational frequency of a CO molecule sufficiently isolated from other CO molecules that dipole–dipole coupling does not occur, the so-called singleton frequency, depends on the electron density on the atom with which CO forms the adsorption complex. In other words, the singleton frequency depends on the degree to which the d orbitals of the metal atom donate electron density to the unoccupied $2\pi^*$ orbital of the adsorbed CO molecule and the degree to which the 5σ orbital of the adsorbed CO donates electron density to the metal atom. Thus, the singleton frequency characterizes the electronic state of the adsorption site.⁴ The dipole–dipole shift at saturation coverage characterizes the size of an ensemble consisting of the same metal atoms, as it is determined by the number of the adjacent vibrating dipoles.⁵

When the metal surface coverage of CO is close to saturation, both the singleton frequency and the dipole–dipole shift can be measured by the isotopic dilution method originally introduced by Hammaker et al.⁴ and then developed in detail by Crossley and King⁵ and Ponc and co-workers.⁶ Essentially, bulk^{4,5,7} and supported metals^{6,8–11} are exposed to $^{13}\text{C}^{16}\text{O} +$

$^{12}\text{C}^{16}\text{O}$ mixtures of varying composition and the vibrational frequency of the adsorbed CO isotopomer is measured as a function of its concentration. Because the vibrational frequencies of $^{12}\text{C}^{16}\text{O}$ and $^{13}\text{C}^{16}\text{O}$ molecules differ by $\sim 50\text{ cm}^{-1}$, the dipole–dipole shift that results from the vibrational interactions between adjacent $^{13}\text{C}^{16}\text{O}$ and $^{12}\text{C}^{16}\text{O}$ species is absent.⁴ Therefore, the frequency of adsorbed $^{13}\text{C}^{16}\text{O}(^{12}\text{C}^{16}\text{O})$ at concentrations sufficiently low that each $^{13}\text{C}^{16}\text{O}(^{12}\text{C}^{16}\text{O})$ molecule is surrounded only by $^{12}\text{C}^{16}\text{O}(^{13}\text{C}^{16}\text{O})$ molecules corresponds to the singleton frequency. The difference between the $^{13}\text{C}^{16}\text{O}(^{12}\text{C}^{16}\text{O})$ band positions at saturation coverage and the singleton frequency is the dipole–dipole shift associated with dipole–dipole interaction between adsorbed $^{13}\text{C}^{16}\text{O}(^{12}\text{C}^{16}\text{O})$ molecules.

Earlier research has shown that a strong intensity redistribution occurs between the bands of $^{13}\text{C}^{16}\text{O}$ and $^{12}\text{C}^{16}\text{O}$ adsorbed on Group VIII noble metals.^{2,4,6,12} Namely, when the difference between vibrational frequencies of the two types of oscillators is relatively small, a redistribution takes place. Essentially, the high-frequency oscillators screen the external electric field at lower frequencies and the absorbance by the low-frequency oscillators is lessened.¹³ In turn, the low-frequency oscillators enhance the external electric field at higher frequencies and hence increase the absorption by the high-frequency oscillators.¹³ In application to infrared (IR) spectroscopy of adsorbed $^{13}\text{C}^{16}\text{O} + ^{12}\text{C}^{16}\text{O}$ mixtures, the redistribution phenomenon results in a suppression in the integral intensity of the $^{13}\text{C}^{16}\text{O}$ band and an enhancement in that of the $^{12}\text{C}^{16}\text{O}$ band relative to the $^{13}\text{C}^{16}\text{O}$ and $^{12}\text{C}^{16}\text{O}$ concentrations on the surface (and, to the same extent, in the gas phase over the sample when adsorption–desorption equilibrium is established). The intensity redistribution and the overlap of the $^{13}\text{C}^{16}\text{O}$ and $^{12}\text{C}^{16}\text{O}$ vibrational bands do not allow a precise determination the $^{13}\text{C}^{16}\text{O}$ band position at low concentrations of $^{13}\text{C}^{16}\text{O}$.

* To whom correspondence should be addressed. Phone: 412-624-9634. Fax: 412-624-9639. E-mail: jdtri@pitt.edu.

[†] N. D. Zelinsky Institute of Organic Chemistry.

[‡] University of Pittsburgh.

The present investigation highlights the utility of using $^{13}\text{C}^{18}\text{O}$ + $^{12}\text{C}^{16}\text{O}$ mixtures rather than $^{13}\text{C}^{16}\text{O}$ + $^{12}\text{C}^{16}\text{O}$ mixtures to probe adsorption sites and the electronic properties of supported metal catalysts, specifically a silica-supported Pt catalyst. The larger difference between the vibrational frequencies of $^{13}\text{C}^{18}\text{O}$ and $^{12}\text{C}^{16}\text{O}$ (100 cm^{-1}) in comparison with the difference between $^{13}\text{C}^{16}\text{O}$ and $^{12}\text{C}^{16}\text{O}$ ($\sim 50\text{ cm}^{-1}$) eliminates the partial overlap of the bands and suppresses the intensity redistribution between the bands of different isotopic molecules in the infrared spectra of adsorbed CO. As a result, three different types of linear CO–Pt complexes have been detected with the $^{13}\text{C}^{18}\text{O}$ + $^{12}\text{C}^{16}\text{O}$ mixtures and characterized by their singleton frequencies and dipole–dipole coupling shifts.

Experimental Section

All of the experiments were conducted with a Pt/SiO₂ catalyst prepared by pore volume impregnation of SiO₂ (Aldrich, 99+%, 60–100 mesh, $300\text{ m}^2\text{ g}^{-1}$, average pore diameter 150 Å) with an aqueous solution of H₂PtCl₆·6H₂O (Alfa, 99.9%), as described elsewhere.¹⁴ The Pt concentration in the impregnation solution was adjusted to obtain a metal loading of 2.4%. The fraction of Pt atoms exposed after reduction at 493 K was 43%, as determined by CO chemisorption.¹⁴ According to transmission electron microscopy (TEM) measurements using a JEM 2010 electron microscope with a resolution of 0.14 nm and accelerating voltage of 200 kV and a previously established procedure,¹⁵ metal particles in the catalyst reduced at 493 K were nearly spherical with an average metal particle size of 2.8 nm. The average particle size was calculated from the measured diameters of approximately 300 particle images in the TEM micrographs.

The IR spectra were recorded with a Research Series II Fourier transform (FT) IR spectrometer (Mattson) equipped with a liquid N₂ cooled MCT detector and an IR cell used in previous research.¹⁶ The cell volume was 200 cm^3 , and the light path length was 15 cm. The cell was equipped with glass stopcocks connected to gas inlet/outlet ports. The spectra of adsorbed CO were measured with resolution of 4 cm^{-1} . To obtain a satisfactory signal-to-noise ratio, 400 scans were accumulated per spectrum.

The IR spectra were collected in the transmission mode, which mandates the use of thin wafers of catalyst. Such self-supporting catalyst wafers ($\sim 20\text{ mg/cm}^2$ thick) were prepared by powdering the catalyst in an agate mortar and then pressing the powder at 830 atm for 3 min. Subsequently, the wafers were mounted into the IR cell, evacuated at room temperature for 15 min, heated to 403 K at 5 K/min, evacuated at 403 K for 1 h, heated to 493 K at 5 K/min in a 5% H₂ + 95% He mixture (both Praxair, 99.999+%) flowing at 80 mL/min, and held at 493 K for 1 h while the gas mixture continued to flow. Finally, the gas phase was evacuated at 493 K to a pressure of 1×10^{-5} Torr.

The frequency shift that results from dipole–dipole coupling and the singleton frequencies of CO adsorbed on the catalyst were measured by the isotopic dilution method^{4,6} using mixtures of different compositions of $^{12}\text{C}^{16}\text{O}$ (Praxair, 99.99+%) with $^{13}\text{C}^{18}\text{O}$ (Isotec, 99+%, ^{13}C , 95+%, ^{18}O) or with $^{13}\text{C}^{16}\text{O}$ (Isotec, 99+%, ^{13}C). Initially, the $^{12}\text{C}^{16}\text{O}$ was adsorbed on a pretreated sample at room temperature and an equilibrium pressure of 12 Torr. Then, the gaseous $^{12}\text{C}^{16}\text{O}$ was evacuated, and a mixture of $^{13}\text{C}^{18}\text{O}$ + $^{12}\text{C}^{16}\text{O}$ or $^{13}\text{C}^{16}\text{O}$ + $^{12}\text{C}^{16}\text{O}$ of known composition (12 Torr) was admitted to the IR cell. After 20 min, the spectrum of adsorbed CO in the presence of the gas phase was recorded. Then, the gaseous CO was evacuated for 20 min, and the

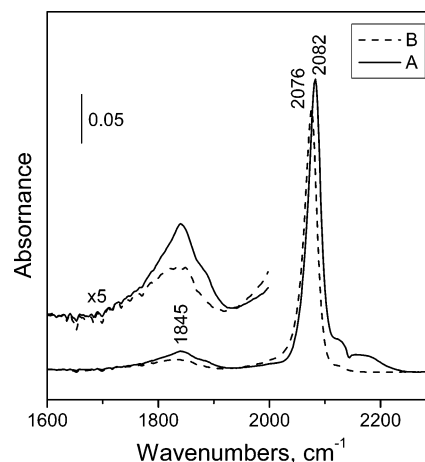


Figure 1. IR spectra of adsorbed $^{12}\text{C}^{16}\text{O}$ at equilibrium pressure of 12 Torr (A) and after subsequent evacuation of the gas phase for 20 min at room temperature (B).

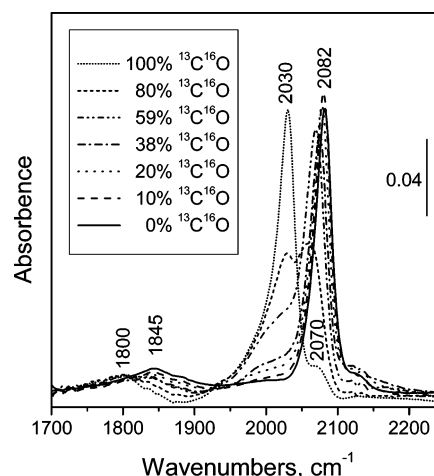


Figure 2. IR spectra of adsorbed $^{13}\text{C}^{16}\text{O}$ + $^{12}\text{C}^{16}\text{O}$ mixtures of different compositions. Spectra were collected at an equilibrium pressure of 12 Torr and room temperature.

spectrum of adsorbed CO was recorded in the absence of gas phase. By repeating this procedure while systematically varying the composition of the isotopic mixture, the spectra of adsorbed CO as a function of $^{13}\text{C}^{18}\text{O}$ + $^{12}\text{C}^{16}\text{O}$ or $^{13}\text{C}^{16}\text{O}$ + $^{12}\text{C}^{16}\text{O}$ mixture composition were determined.

Results

For the Pt/SiO₂ catalyst reduced at 493 K, the addition of $^{12}\text{C}^{16}\text{O}$ at room-temperature resulted in IR bands at 1845 and 2082 cm^{-1} (Figure 1).¹⁷ These bands are assigned to CO adsorbed on metallic Pt in the bridging and the linear forms, respectively.¹⁸ When the gas phase was removed by evacuation at room temperature, the intensity of the 1845 cm^{-1} band decreased by a factor of ~ 2 , with the peak maximum position remaining constant. The intensity of the band at 2082 cm^{-1} decreased by approximately 10%, and the peak maximum shifted to 2076 cm^{-1} . Subsequent exposure of the Pt/SiO₂ wafer to 100% $^{13}\text{C}^{16}\text{O}$ resulted in a spectrum that consisted of an intense band at 2030 cm^{-1} and a low-intensity broad band at 1800 cm^{-1} ; the bands are assigned to $^{13}\text{C}^{16}\text{O}$ molecules adsorbed on metallic Pt in the linear and the bridging forms, respectively (Figure 2). Additionally, there was a low-intensity band at 2070 cm^{-1} that most likely belongs to linear complexes of $^{12}\text{C}^{16}\text{O}$ with Pt.¹⁹

When the $^{13}\text{C}^{16}\text{O}$ concentration in the gas mixture was 80%, the spectrum of CO adsorbed on Pt consisted of two vibrational

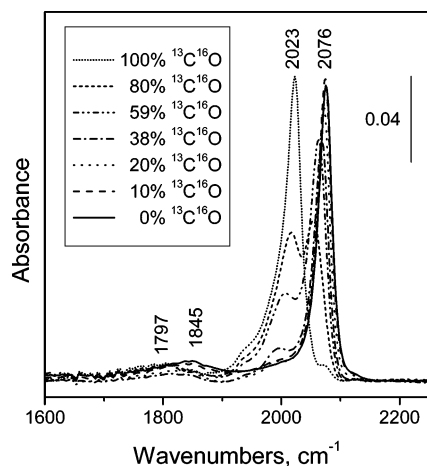


Figure 3. IR spectra of adsorbed $^{13}\text{C}^{16}\text{O} + ^{12}\text{C}^{16}\text{O}$ mixtures of different compositions. Carbon monoxide adsorption was performed at equilibrium pressure of 12 Torr. Spectra were collected after the gas phase was removed by evacuation for 20 min at room temperature.

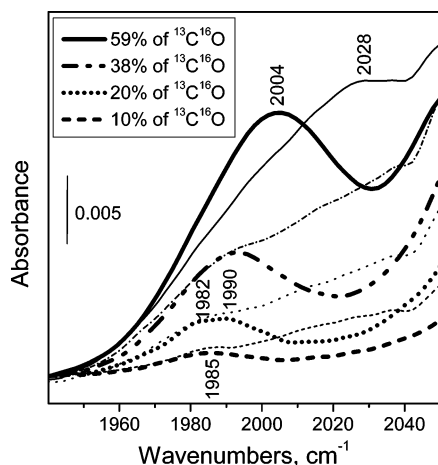


Figure 4. IR spectra of linear $^{13}\text{C}^{16}\text{O}$ -Pt complexes after adsorption of $^{13}\text{C}^{16}\text{O} + ^{12}\text{C}^{16}\text{O}$ mixtures ($P_{\text{total}} = 12$ Torr) of different compositions after subtraction of the $^{12}\text{C}^{16}\text{O}$ contribution. Spectra were collected in the presence (thin lines) and in the absence (thick lines) of gas phase.

bands with maxima at 2030 ($^{13}\text{C}^{16}\text{O}$ -Pt) and 2060 cm^{-1} ($^{12}\text{C}^{16}\text{O}$ -Pt). The intensity of the $^{12}\text{C}^{16}\text{O}$ -Pt band was higher than that of $^{13}\text{C}^{16}\text{O}$ -Pt. At $^{13}\text{C}^{16}\text{O}$ concentrations less than 60%, the spectrum of linear complexes consisted of an intense band at 2070–2082 cm^{-1} that corresponds to $^{12}\text{C}^{16}\text{O}$ -Pt complexes. The band of linear $^{13}\text{C}^{16}\text{O}$ -Pt complexes was detected only as a shoulder on the low-frequency side of the 2070–2082 cm^{-1} band.

After the catalyst wafer with preadsorbed $^{13}\text{C}^{16}\text{O} + ^{12}\text{C}^{16}\text{O}$ mixture was evacuated at room temperature for 20 min, the band attributed to the linear $^{13}\text{C}^{16}\text{O}$ -Pt species was observed at $^{13}\text{C}^{16}\text{O}$ concentrations as low as 20% (Figure 3). After subtraction of the adsorbed $^{12}\text{C}^{16}\text{O}$ spectrum from each spectrum of the adsorbed $^{13}\text{C}^{16}\text{O} + ^{12}\text{C}^{16}\text{O}$ mixture when the gas phase had been evacuated, the $^{13}\text{C}^{16}\text{O}$ -Pt band was still detectable at a $^{13}\text{C}^{16}\text{O}$ concentration of 10% (Figure 4).²⁰ At this concentration, the position of the $^{13}\text{C}^{16}\text{O}$ band maximum was 1985 cm^{-1} , and the band was relatively broad. After the catalyst was exposed to an isotopic mixture containing 20% $^{13}\text{C}^{16}\text{O}$ and subsequently evacuated, the band at 1985 cm^{-1} split into two poorly resolved bands at 1982 and 1990 cm^{-1} (Figure 4). Apparently, the band at 1985 cm^{-1} is an unresolved superimposition of the bands at 1982 and 1990 cm^{-1} , and thus, the frequency of 1982 cm^{-1} should be considered the singleton of $^{13}\text{C}^{16}\text{O}$ linearly adsorbed

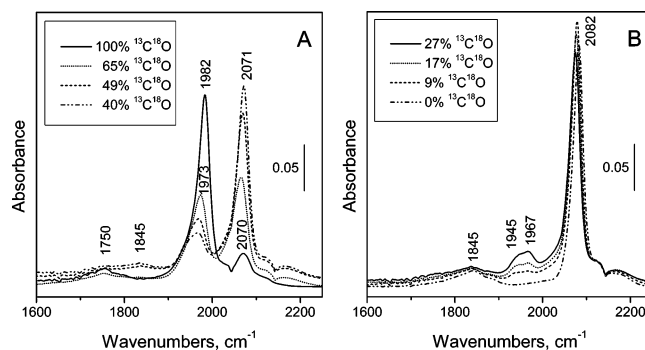


Figure 5. IR spectra of adsorbed $^{13}\text{C}^{18}\text{O} + ^{12}\text{C}^{16}\text{O}$ mixtures of different compositions. Spectra were collected at an equilibrium pressure of 12 Torr and room temperature.

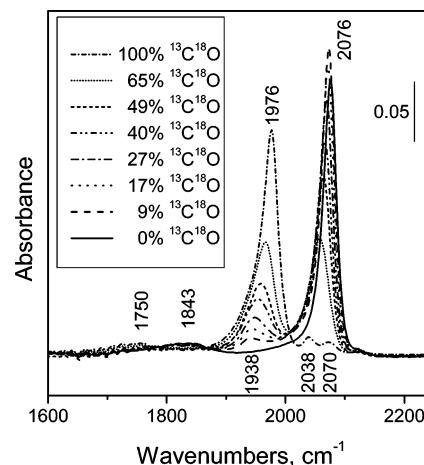


Figure 6. IR spectra of adsorbed $^{13}\text{C}^{18}\text{O} + ^{12}\text{C}^{16}\text{O}$ mixtures of different compositions. Carbon monoxide adsorption was performed at equilibrium pressure of 12 Torr. Spectra were collected after the gas phase was removed by evacuation for 20 min at room temperature.

on Pt. Exposure to 38% $^{13}\text{C}^{16}\text{O}$ in the mixture and subsequent evacuation resulted in a spectrum consisting of a single band at 1993 cm^{-1} . The maximum frequency shifted from 1993 to 2023 cm^{-1} as the concentration of $^{13}\text{C}^{16}\text{O}$ in the mixture was increased from 38 to 100% (Figures 3 and 4). When gas-phase CO was present, the spectra of adsorbed $^{13}\text{C}^{16}\text{O}$ contained a broad band at 2000–2030 cm^{-1} (Figure 4). This band disappeared when gas phase was evacuated.

The spectra of $^{13}\text{C}^{18}\text{O} + ^{12}\text{C}^{16}\text{O}$ mixtures with varying compositions adsorbed on Pt/SiO₂ measured in the presence of the gaseous phase and after evacuation are shown in Figures 5 and 6, respectively. With a $^{13}\text{C}^{18}\text{O}$ concentration in the adsorption mixture between 9 and 40%, the spectrum of linear $^{13}\text{C}^{18}\text{O}$ -Pt species in the presence of the gas phase consisted of two poorly resolved bands at ~ 1945 and 1967 cm^{-1} . At $^{13}\text{C}^{18}\text{O}$ concentrations in the mixture greater than 40%, the spectrum of the linear $^{13}\text{C}^{18}\text{O}$ -Pt complexes consisted of a single band with a frequency maximum that increased from 1968 cm^{-1} (50% of $^{13}\text{C}^{18}\text{O}$) to 1982 cm^{-1} ($\sim 100\%$ of $^{13}\text{C}^{18}\text{O}$) (Figure 5).

Increasing the concentration of $^{13}\text{C}^{18}\text{O}$ in the gaseous mixture resulted in a decrease in the intensity of the linear $^{12}\text{C}^{16}\text{O}$ -Pt band at 2082 cm^{-1} and to a shift in position to lower frequencies. With 65% $^{13}\text{C}^{18}\text{O}$ in the gaseous mixture, the position of the linear $^{12}\text{C}^{16}\text{O}$ -Pt band was at 2065 cm^{-1} (Figure 5). When the $^{13}\text{C}^{18}\text{O}$ concentration was near 100%, the spectrum of adsorbed $^{12}\text{C}^{16}\text{O}$ consisted of a single band at 2070 cm^{-1} (ref 21) (Figure 5), which may correspond to the singleton frequency of a linear complex of $^{12}\text{C}^{16}\text{O}$ with electron deficient $\text{Pt}^{\delta+}$.²² The 2070- cm^{-1} band was not observed at lower concentrations of $^{13}\text{C}^{18}\text{O}$

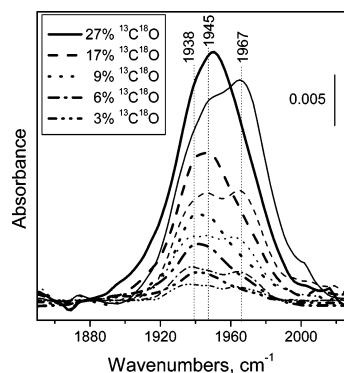


Figure 7. IR spectra of linear $^{13}\text{C}^{18}\text{O}$ –Pt complexes after adsorption of $^{13}\text{C}^{18}\text{O} + ^{12}\text{C}^{16}\text{O}$ mixtures ($P_{\text{total}} = 12$ Torr) of different compositions after subtraction of the $^{12}\text{C}^{16}\text{O}$ contribution. Spectra were collected in the presence (thin lines) and in the absence (thick lines) of gas phase.

because it was masked by the intense band of the linear $^{12}\text{C}^{16}\text{O}$ –Pt complexes at 2065–2085 cm^{-1} .

When the $^{13}\text{C}^{18}\text{O}$ concentration in the gas mixture was increased, the 1845 cm^{-1} band corresponding to bridged $^{12}\text{C}^{16}\text{O}$ on Pt decreased in intensity. Simultaneously, the intensity of a new band at 1750 cm^{-1} , attributed to bridging complexes of $^{13}\text{C}^{18}\text{O}$ with Pt, increased (Figure 5).

After evacuation of the gas-phase CO from the IR cell at room temperature, the 1967 cm^{-1} band of the linear $^{13}\text{C}^{18}\text{O}$ –Pt complexes disappeared. The spectrum of linear $^{13}\text{C}^{18}\text{O}$ –Pt when the $^{13}\text{C}^{18}\text{O}$ concentration was 9% consisted of a single band at 1938 cm^{-1} (Figure 6), the singleton frequency of $^{13}\text{C}^{18}\text{O}$ –Pt. When the $^{13}\text{C}^{18}\text{O}$ concentration was close to 100%, the band of the linear $^{13}\text{C}^{18}\text{O}$ –Pt complexes shifted toward 1976 cm^{-1} and new bands appeared at 2038 and 2070 cm^{-1} (Figure 6). The 2038 cm^{-1} band corresponds to the singleton frequency of linear $^{12}\text{C}^{16}\text{O}$ complexes with metallic Pt, whereas the 2070 cm^{-1} band,²¹ as already mentioned, is most likely the singleton of linear complexes of $^{12}\text{C}^{16}\text{O}$ with $\text{Pt}^{\delta+}$.²² The difference in the singleton frequencies of $^{12}\text{C}^{16}\text{O}$ –Pt (2038 cm^{-1}) and $^{13}\text{C}^{18}\text{O}$ –Pt (1938 cm^{-1}) was 100 cm^{-1} , a value that coincides with the difference in the C–O bond vibration frequencies of gas-phase $^{12}\text{C}^{16}\text{O}$ and $^{13}\text{C}^{18}\text{O}$ molecules.

The spectra of linear $^{13}\text{C}^{18}\text{O}$ –Pt complexes at low concentrations of $^{13}\text{C}^{18}\text{O}$ in the $^{13}\text{C}^{18}\text{O} + ^{12}\text{C}^{16}\text{O}$ mixtures were obtained by subtraction of the spectrum of adsorbed $^{12}\text{C}^{16}\text{O}$ from the spectra of adsorbed mixtures (Figure 7). The vibrations associated with the $^{13}\text{C}^{18}\text{O}$ –Pt complexes were detected at $^{13}\text{C}^{18}\text{O}$ concentrations as low as 3%. It is reasonable to suggest that, at such a low concentration, the dipole–dipole interaction between adsorbed $^{13}\text{C}^{18}\text{O}$ molecules is negligible. Thus, when the gas-phase was present, the bands at 1938, 1945, and 1967 cm^{-1} (Figure 7) were attributed to the singleton frequencies of three different linear $^{13}\text{C}^{18}\text{O}$ –Pt adsorption complexes on the metallic Pt surface. An increase in the coverage of $^{13}\text{C}^{18}\text{O}$ resulted in an increase in the intensities of each of the three bands. The largest intensity increase was observed for the 1967 cm^{-1} band and the smallest for 1938 cm^{-1} band. However, at $^{13}\text{C}^{18}\text{O}$ concentrations $\geq 40\%$ the two low-frequency bands transformed into the high-frequency band because of intensity redistribution (Figure 5).

After evacuation of the gas phase, the 1967 cm^{-1} band disappeared. However, the total intensity of the bands at 1938 and 1945 cm^{-1} actually increased. And increasing the $^{13}\text{C}^{18}\text{O}$ concentration increased the intensity of the 1945 cm^{-1} band more than that of the band at 1938 cm^{-1} . The band intensities were comparable at a $^{13}\text{C}^{18}\text{O}$ concentration of 17%. At higher

$^{13}\text{C}^{18}\text{O}$ concentrations, the spectrum consisted of only one band with the maximum that shifted from 1950 cm^{-1} (27% of $^{13}\text{C}^{18}\text{O}$) (Figure 7) to 1976 cm^{-1} ($\sim 100\%$ of $^{13}\text{C}^{18}\text{O}$) due to dipole–dipole interaction (Figure 6).

Discussion

The spectrum evolution of CO adsorbed on Pt/SiO₂ that occurs when isotopic ratios of $^{13}\text{C}^{16}\text{O} + ^{12}\text{C}^{16}\text{O}$ and $^{13}\text{C}^{18}\text{O} + ^{12}\text{C}^{16}\text{O}$ mixtures are varied demonstrates a fast isotopic exchange between gaseous CO and CO adsorbed on metallic platinum (Figures 2, 3, 5, and 6). Because the number of gaseous CO molecules in the IR cell ($\sim 8.5 \times 10^{19}$) greatly exceeds the number of Pt atoms in the sample ($\sim 3 \times 10^{17}$), it can be concluded that the isotopic composition of the CO adsorption layers on Pt is similar to that of the gaseous $^{13}\text{C}^{16}\text{O} + ^{12}\text{C}^{16}\text{O}$ and $^{13}\text{C}^{18}\text{O} + ^{12}\text{C}^{16}\text{O}$ mixtures when isotopic equilibrium is reached. And this conclusion is utilized in the interpretation of the other results of this investigation.

One form of CO is weakly adsorbed on Pt at high metal surface coverage, as indicated by the small ($\sim 6 \text{ cm}^{-1}$) shift to a lower frequency of the band attributed to linear $^{12}\text{C}^{16}\text{O}$ –Pt complexes as well as by the decrease in the band intensities of CO adsorbed on Pt in the linear and bridging forms that occurs after evacuation of the catalyst wafer with preadsorbed CO at room temperature (Figure 1). This interpretation is in agreement with a calorimetric study of CO adsorption on Pt/SiO₂ at 673 K²³ in which an equilibrium existed between gaseous CO molecules and those adsorbed on the metal surface. At low CO coverages on Pt, the heat of CO adsorption is 180–190 kJ mol^{-1} , and it gradually decreases with increasing CO coverage to 75 kJ mol^{-1} at a coverage of 0.7 monolayer (ML). When the heat of adsorption is 75 kJ mol^{-1} , the rate constant for the CO desorption from Pt is of the order of $\sim 1 \text{ s}^{-1}$ assuming the first-order desorption kinetics and a pre-exponential factor of 10^{13} s^{-1} . Therefore, at coverages close to saturation (0.6–0.7 ML), an equilibrium between gas-phase CO and CO adsorbed on Pt is rapidly established, even at room temperature. Most likely, the weakly adsorbed CO on Pt facilitates the isotopic equilibration between gaseous and adsorbed CO molecules.

With the gas-phase present, the linear $^{13}\text{C}^{16}\text{O}$ –Pt complexes are detected only with $^{13}\text{C}^{16}\text{O} + ^{12}\text{C}^{16}\text{O}$ mixtures containing more than 50% of $^{13}\text{C}^{16}\text{O}$ (Figure 2). A similar phenomenon was observed previously for $^{13}\text{C}^{16}\text{O} + ^{12}\text{C}^{16}\text{O}$ mixtures adsorbed on Pt single crystals²⁴ and on Pt supported on alumina.⁶ The observance of the linear $^{13}\text{C}^{16}\text{O}$ –Pt complexes only with mixture containing predominantly $^{13}\text{C}^{16}\text{O}$ is the result of an intensity redistribution between the band of $^{13}\text{C}^{16}\text{O}$ –Pt and the band of $^{12}\text{C}^{16}\text{O}$ –Pt. A theoretical interpretation of this intensity redistribution effect was given by King²⁵ and Persson et al.^{2,26}

The intensity redistribution effect is clearly observed in the spectra of adsorbed $^{13}\text{C}^{16}\text{O} + ^{12}\text{C}^{16}\text{O}$ mixtures after evacuation of the gas phase. The effect is evident from the fact that with 80% $^{13}\text{C}^{16}\text{O}$ in the mixture, the band intensity of the $^{12}\text{C}^{16}\text{O}$ –Pt complex (2055 cm^{-1}) is higher than that of $^{13}\text{C}^{16}\text{O}$ –Pt species (Figure 3). The spectra of adsorbed species are better resolved in the absence of gas phase, and the $^{13}\text{C}^{16}\text{O}$ –Pt complex is detected when the adsorbed mixture contains $\sim 10\%$ of $^{13}\text{C}^{16}\text{O}$ (Figure 4). The existence of weakly adsorbed CO on the Pt surface, characterized by a broad band with a maximum at 2000–2030 cm^{-1} (Figure 4), accounts for the strong influence of the gas phase on the spectra of adsorbed mixtures.

The Pt sites associated with the strongly adsorbed CO are inhomogeneous. This is inferred from the spectra of adsorbed

CO shown in Figure 4. In the absence of the gas phase, the spectrum of $^{13}\text{C}^{16}\text{O}$ -Pt with a mixture containing 20% $^{13}\text{C}^{16}\text{O}$ consists of two bands with maxima at 1982 and 1990 cm^{-1} (Figure 4). At higher $^{13}\text{C}^{16}\text{O}$ concentrations in the mixture, an intensity redistribution occurs between the 1982 and 1990 cm^{-1} bands that results in a significant increase in the 1990 cm^{-1} band intensity. This phenomenon indicates that these different sites of CO adsorption are in close vicinity; videlicet, they are located on the same metallic particle.

An intensity redistribution also occurs for $^{13}\text{C}^{18}\text{O} + ^{12}\text{C}^{16}\text{O}$ mixtures adsorbed on silica-supported Pt, but the intensity redistribution between the bands of linear $^{13}\text{C}^{18}\text{O}$ -Pt and $^{12}\text{C}^{16}\text{O}$ -Pt adsorption complexes is much weaker than that between the bands of $^{13}\text{C}^{16}\text{O}$ -Pt and $^{12}\text{C}^{16}\text{O}$ -Pt. For example, the $^{13}\text{C}^{18}\text{O}$ -Pt and $^{12}\text{C}^{16}\text{O}$ -Pt band intensities are approximately equal at a $^{13}\text{C}^{18}\text{O}$ concentration of 65% and a $^{12}\text{C}^{16}\text{O}$ concentration of 35% (Figures 5 and 6), while the band intensity of the $^{13}\text{C}^{16}\text{O}$ -Pt complex is lower than that of the $^{12}\text{C}^{16}\text{O}$ -Pt even at a $^{13}\text{C}^{16}\text{O}$ concentration of 80% and only 20% $^{12}\text{C}^{16}\text{O}$ (Figure 3). These differences in intensity are most likely because the vibrational frequency difference between $^{13}\text{C}^{18}\text{O}$ and $^{12}\text{C}^{16}\text{O}$ is two times larger than that between $^{13}\text{C}^{16}\text{O}$ and $^{12}\text{C}^{16}\text{O}$. As a result of a weaker intensity redistribution effect between the $^{13}\text{C}^{18}\text{O}$ -Pt and $^{12}\text{C}^{16}\text{O}$ -Pt bands, the linear $^{13}\text{C}^{18}\text{O}$ -Pt complexes are detectable in the spectra of adsorbed $^{13}\text{C}^{18}\text{O} + ^{12}\text{C}^{16}\text{O}$ mixtures containing only $\sim 3\%$ of $^{13}\text{C}^{18}\text{O}$, both in the presence and absence of the gas phase (Figure 7).

In the presence of a gas phase with a low concentration of $^{13}\text{C}^{18}\text{O}$, the spectrum of $^{13}\text{C}^{18}\text{O}$ adsorbed on metallic Pt consists of three bands: 1938, 1945, and 1967 cm^{-1} . These three bands correspond to the singleton frequencies of different linear complexes of $^{13}\text{C}^{18}\text{O}$ with metallic Pt. The decrease in the 1967 cm^{-1} band intensity during evacuation results in an increase in the total intensity of 1938 and 1945 cm^{-1} bands (Figure 7). Most likely the removal of the weakly adsorbed linear CO complexes results in the conversion of some bridging complexes into the linear species. This interpretation is consistent with the larger intensity decrease of the band associated with bridging species at 1845 cm^{-1} than that of linear complexes at ~ 2082 cm^{-1} that result from evacuation of gas-phase CO (Figure 1). Transformation of bridging CO complexes into linear species as CO coverage decreased has been shown by high-resolution electron energy loss spectroscopy and low-energy electron diffraction investigations with a Pt(111) single crystal.²⁷ It is also possible that the increase in the total intensity of the 1938 and 1945 cm^{-1} bands after removal of the 1967- cm^{-1} band by evacuation (Figure 7) is due to an intensity redistribution between the lower frequency bands and the band at 1967 cm^{-1} . However, this possibility can be ruled out because an intensity increase in the 1938 and 1945 cm^{-1} bands is observed at low $^{13}\text{C}^{18}\text{O}$ concentrations (Figure 7) when lateral interactions between $^{13}\text{C}^{18}\text{O}$ molecules are negligible.

As the $^{13}\text{C}^{18}\text{O}$ concentration in the isotopic mixture is increased, the intensity of the 1945 cm^{-1} band increases faster than that of the 1938 cm^{-1} band (Figure 7). This is likely a result of an intensity redistribution between those bands. As an intensity redistribution occurs between the bands at 1938, 1945, and 1967 cm^{-1} , all three kinds of linear complexes are located in close vicinity, videlicet, on the same metallic particle.

The intensity redistribution between the low-frequency and high-frequency bands corresponding to different linear $^{13}\text{C}^{18}\text{O}$ -Pt complexes makes it difficult to determine precisely the dipole-dipole shifts. Indeed, at high $^{13}\text{C}^{18}\text{O}$ concentrations in the $^{13}\text{C}^{18}\text{O} + ^{12}\text{C}^{16}\text{O}$ mixtures, the 1938 and 1945 cm^{-1} bands

convert into the 1967 cm^{-1} band of $^{13}\text{C}^{18}\text{O}$ that is weakly adsorbed in linear form on Pt (in the presence of the gas phase). Therefore, from the band maximum at 1982 cm^{-1} attributed to $^{13}\text{C}^{18}\text{O}$ -Pt complexes that result from adsorption of 100% of $^{13}\text{C}^{18}\text{O}$ and the singleton frequency, the dipole-dipole shift can be determined only for $^{13}\text{C}^{18}\text{O}$ weakly adsorbed on Pt. This form of adsorption is characterized by a singleton frequency of 1967 cm^{-1} and a dipole-dipole shift of 15 cm^{-1} . In the absence of the gas phase the dipole-dipole shift can be determined only for $^{13}\text{C}^{18}\text{O}$ -Pt complexes characterized by the singleton frequency of 1945 cm^{-1} . For those $^{13}\text{C}^{18}\text{O}$ -Pt complexes the dipole-dipole shift is equal to 31 cm^{-1} . This value is 16 cm^{-1} larger than that for the weakly bound $^{13}\text{C}^{18}\text{O}$ -Pt complexes characterized by the 1967 cm^{-1} singleton. The dipole-dipole shift for the $^{13}\text{C}^{18}\text{O}$ -Pt band at 1938 cm^{-1} cannot be determined because at higher $^{13}\text{C}^{18}\text{O}$ concentrations the intensity of the 1938 cm^{-1} band becomes negligible due to the intensity redistribution between the bands at 1938 and 1945 cm^{-1} . Thus, the contribution of the band at 1938 cm^{-1} to the CO band at $^{13}\text{C}^{18}\text{O}$ saturation coverage cannot be ascertained.

It is worth mentioning that the difference between the maximum band frequencies of linearly adsorbed $^{13}\text{C}^{18}\text{O}$ and $^{12}\text{C}^{16}\text{O}$ in the presence (1982 and 2082 cm^{-1}) and in the absence (1976 and 2076 cm^{-1}) of the gas phase, as well as the difference between the singleton frequency of $^{13}\text{C}^{18}\text{O}$ -Pt (1938 cm^{-1}) and $^{12}\text{C}^{16}\text{O}$ -Pt (2038 cm^{-1}), are equal to 100 cm^{-1} . This value corresponds to the frequency difference between the vibrations of gas-phase $^{13}\text{C}^{18}\text{O}$ and $^{12}\text{C}^{16}\text{O}$ molecules. Therefore, for the $^{13}\text{C}^{18}\text{O}$ -Pt complexes the singleton frequency and dipole-dipole shift can be determined in a single experiment with a very low concentration of $^{13}\text{C}^{18}\text{O}$ in the $^{13}\text{C}^{18}\text{O} + ^{12}\text{C}^{16}\text{O}$ mixture. In this situation, the dipole-dipole shift is the difference between the $^{13}\text{C}^{18}\text{O}$ -Pt band position and that of the $^{12}\text{C}^{16}\text{O}$ -Pt band reduced by 100 cm^{-1} . Naturally, for the $^{12}\text{C}^{16}\text{O}$ -Pt complexes the dipole-dipole shift will be the same as for the $^{13}\text{C}^{18}\text{O}$ -Pt, while the singleton frequency will exceed that of $^{13}\text{C}^{18}\text{O}$ -Pt by 100 cm^{-1} .

The nature of the different linear CO-Pt complexes is also worth considering. The most thermodynamically stable crystallographic face of Pt is the (111) surface.²⁸ Some experimental observations provide evidence that the surface of supported Pt particles may consist predominantly of the Pt(111) face, even though the structural characterization data for supported Pt particles of few nanometers in size are not available. For example, the maximum CO coverage of Pt in Pt/SiO₂ and in Pt(111) is the same: 0.7 ML.^{23,25,26,29-31} Moreover, the initial heat of CO adsorption and the dependence of the heat of adsorption on the metal surface coverage are also similar for Pt/SiO₂ and Pt(111).^{23,32} Nevertheless, it has to be recognized that for an actual supported catalysts one cannot expect the exclusive formation of ideally shaped particles such as tetrahedrons with (111) faces. Within the accuracy of the TEM instrument employed in this investigation, the metal particles on the support surface appear nearly spherical. In other words, the particle surface is curved. Obviously, the curvature is provided by combination of terraces (probably, mainly of the (111) structure), steps, and kinks. The smaller the particle radius, the greater the density of steps and kinks and, as a consequence, the higher concentration of adsorption sites located thereat.

Thus, there are at least three types of adsorption sites for CO on the surface of a supported Pt particle: sites on terraces and sites on edges and corners of the steps and kinks. However, there is no reason to expect that any of these sites will bind CO weakly.

When the CO coverage of Pt is high, a compression of the adsorbed CO layer takes place.^{27,33–36} In the compressed adlayer the adsorbed CO molecules are located so close to each other that their orbitals overlap. This leads to an intermolecular repulsion that results in an electron density withdrawal from $2\pi^*$ orbitals. And the electron density withdrawal results in a strengthening of C–O bond and a weakening of Pt–C bond. Hence, the frequency of the C–O bond vibration increases, and the heat of CO adsorption decreases. Thus, the CO molecules weakly adsorbed on Pt that are characterized by the band at 1967 cm^{-1} (Figure 7) should be located deeply inside the CO adlayer on (111) terraces. It is worth noting that weakly bound CO species for silica- and alumina-supported Pt have been previously reported,^{29,37,38} but no interpretation of the weak Pt–CO bonding was provided.

The strongly bound CO species characterized by the band located at 1938 cm^{-1} (Figure 7) is assigned to CO adsorbed at corners and edges of the steps while the band at 1945 cm^{-1} (Figure 7) is attributed to CO molecules located at the periphery of the compressed CO islands on the terraces. Investigations with single crystals have shown that terrace and step sites can be distinguished by infrared spectroscopy of adsorbed CO. Specifically, the vibrational frequency of CO adsorbed on corners and steps is approximately 20 cm^{-1} lower than when it is adsorbed on terraces.^{39–43} In addition, no difference is observed between the frequencies of CO adsorbed on step and kink sites of a Pt crystal with (111) terraces and (100) steps (Pt(533)) and of a crystal with (111) terraces and kinked steps (Pt(432)).⁴⁰

There are several reasons to exclude the possibility that the band at 1938 cm^{-1} (Figure 7) is associated with CO adsorbed on (100) terraces. First, the catalyst reduction temperature (493 K) was too low to expect the formation of well-crystallized cuboctahedral Pt particles with (100) and (111) faces. Second, irregularly shaped particles as small as 2.8 nm in size should have relatively high density of defects, which would manifest themselves in the spectra of adsorbed CO and hence support the assignment of the 1938 cm^{-1} band to those corners and edges, as described above. Third, the singleton frequencies determined by the isotopic dilution method with $^{13}\text{C}^{16}\text{O} + ^{12}\text{C}^{16}\text{O}$ mixtures for $^{12}\text{C}^{16}\text{O}$ adsorbed on the Pt(100) and Pt(111) surfaces are 2062 and 2065 cm^{-1} , respectively.²⁵ The difference between these singletons is much less than between the singletons of the two strongly bound CO modes at 1938 and 1945 cm^{-1} . (The difference of $\sim 20\text{ cm}^{-1}$ between CO adsorbed on steps and terraces was observed in investigations with Pt single crystals.^{39–43}) Thus, if two different linear CO modes are detected for the same Pt particle, it is more likely for them to belong to the CO species adsorbed on terraces and defect sites than to the species on the (100) and (111) terraces.

There are many IR investigations of CO adsorption on supported Pt.^{18,39,40,44,55} For the supports that do not interact strongly with the metal particles such as silica, carbon, or alumina, several studies reported more than one linear CO adsorption mode.^{40,45,47–49,52,54,55} However, the different linear CO adsorption modes were attributed to CO adsorption on terraces and steps in only a few of these investigations.^{40,45,52} Usually, these modes are assigned to CO adsorbed on Pt sites located far from and at the Pt/support interface.^{47,48,54} They are also assigned to CO adsorbed on particles of the different size⁵⁵ as it was established for supported Pt catalysts that there is a correlation between the vibrational frequency of linear CO mode and the metal particle size.^{49,50}

Thus, it is critical when assigning bands of CO linearly adsorbed on Pt particles to the adsorption complexes located on terraces and steps to verify that the different adsorption sites are located in close vicinity, in other words, on the same particle. However, such verification is absent in the published investigations that attribute the bands in IR spectra of adsorbed CO to the adsorption on terraces and steps.^{40,45,52} Moreover, it is inferred from the results of several different research investigations^{40,45,52} that two⁴⁵ or three^{40,52} bands in the IR spectra of CO adsorbed on Pt in the linear mode may not be associated with CO adsorption on terraces and steps, but rather are artifacts due to coverage effects.

Multiple bands have been reported elsewhere at coverages far below saturation.^{40,45,52} It has been shown for a Pt/SiO₂ catalyst²³ that at low CO pressures the adsorption process takes place chromatographically. Namely, CO saturates the Pt particles in the order in which contact with gaseous CO occurs, which creates a distribution of coverages for the Pt particles in the sample. Different coverages result in a different position of the CO vibrational band because of the coverage dependent dipole–dipole coupling shift. Thus, under conditions in which there is a CO coverage distribution coupled with a Pt particle size distribution several CO absorption bands may be present even if all CO molecules are adsorbed on similar sites.

The results of a study by Rasko⁵² with a 1% Pt/SiO₂ catalyst are, in fact, consistent with the suggestion that multiple linear CO adsorption modes are due to the coverage distribution effect rather than CO adsorption on monatomic Pt⁰, edge, and kinked Pt atoms as suggested by the author. After 20 h exposure of the catalyst to 10 Torr CO, three bands initially positioned at 2107 , 2069 , and 2045 cm^{-1} converted into a single band at 2069 cm^{-1} . This result supports the interpretation that the equilibration of the CO coverage over different Pt particles results in a uniform dipole–dipole coupling shift and, hence, a single CO absorption band. Further support for the suggestion that the sites characterized by the bands at 2107 , 2069 , and 2045 cm^{-1} are not located on the same particle can be gleaned from an analysis of the band intensities. The band at 2045 cm^{-1} attributed to CO adsorbed on kinked Pt atoms has the highest intensity at a CO pressure of 0.01 Torr. Taking the intensity redistribution effect into consideration would require the surface of the Pt particles to consist mainly of kinked sites, which is unrealistic. The suggestion that at low coverages kinked sites are preferentially filled can be ruled out by chromatographic character of CO adsorption.²³ Similarly, the two bands at 2078 and 2041 cm^{-1} detected for a 5% Pt/Al₂O₃⁵² may not be associated with CO adsorption on edges and kinked sites comprised of Pt atoms but rather a result of coverage effect. However, the band at 2117 cm^{-1} also observed after exposure of the 5% Pt/Al₂O₃ catalyst to CO⁵² is most likely not due to CO adsorbed on Pt⁰ moieties but due to CO adsorbed on Pt atoms electronically perturbed by the alumina support.^{47,48,54}

In another investigation, IR bands at 2081 , 2070 , and 2063 cm^{-1} were observed after exposure of silica-supported Pt catalysts of different dispersion to CO.⁴⁰ These bands were assigned to CO linearly bonded to face, corner, and edge sites of the Pt particles. However, a dipole–dipole coupling shift as low as 6 cm^{-1} when the CO coverage increased from 0 to 80% suggests that these bands may be an artifact associated with both a CO coverage distribution resulting from CO adsorption by dosing and a particle size distribution, as the frequency of the CO absorption band is also a function of Pt particle size.^{49,50} Typically, the dipole–dipole coupling shift for CO strongly bound to Pt determined from experiments with CO isotopic

mixtures at saturation coverage is between 30 and 40 cm⁻¹. A value of 31 cm⁻¹ was obtained for the silica-supported Pt used in this investigation, while approximately 35 cm⁻¹ and approximately 39 cm⁻¹ were observed for Pt(111) and Pt(100) surfaces²⁵ and for alumina-supported Pt,⁷ respectively.

Conclusion

The adsorption of ¹³C¹⁸O + ¹²C¹⁶O and ¹³C¹⁶O + ¹²C¹⁶O mixtures on a silica-supported Pt catalyst has been investigated. With ¹³C¹⁸O + ¹²C¹⁶O mixtures, no overlap between absorption bands of the different isotopic CO molecules adsorbed on the metal was observed. In addition, the larger difference between the vibrational frequencies for the bands of ¹³C¹⁸O and ¹²C¹⁶O (100 cm⁻¹) than between ¹³C¹⁶O and ¹²C¹⁶O (~50 cm⁻¹) significantly suppresses the degree of intensity redistribution between ¹³C¹⁸O and ¹²C¹⁶O vibrating dipoles. As a result of the decreased intensity redistribution, the band of adsorbed ¹³C¹⁸O is detectable at concentrations as low as 3% when the dipole–dipole interaction between adsorbed ¹³C¹⁸O molecules is negligible. Thus, both the singleton frequency and the dipole–dipole shift can be determined in a single experiment. In the absence of a dipole–dipole interaction, the singleton frequency coincides with the position of the vibrational band of adsorbed ¹³C¹⁸O, whereas the dipole–dipole shift is the difference between the band position of adsorbed ¹²C¹⁶O and the ¹³C¹⁸O singleton frequency decreased by 100 cm⁻¹ (the difference between the ¹³C¹⁸O and the ¹²C¹⁶O vibrational frequencies).

Three different linear CO–Pt adsorption complexes were identified with ¹³C¹⁸O singleton frequencies of 1938, 1945, and 1967 cm⁻¹. The adsorption band at 1967 cm⁻¹ is a mode associated with CO that is adsorbed weakly on the Pt surface and is removed by evacuation of the catalyst wafer at room temperature. An intensity redistribution occurs between these bands with a relatively high ¹³C¹⁸O concentration in the ¹³C¹⁸O + ¹²C¹⁶O mixture, indicating that all three types of adsorption complexes are located in close vicinity, namely, on the same metal particle. The intensity redistribution between the 1938 and 1945 cm⁻¹ bands does not allow determination of the dipole–dipole shift for the lower frequency band. The weakly adsorbed CO mode (band at 1967 cm⁻¹) is attributed to the molecules located deeply inside of the CO adlayer on the (111) terraces of Pt particles, while the stronger adsorbed CO molecules are located at the steps (1938 cm⁻¹) and (111) terraces in the periphery of the compressed CO islands (1945 cm⁻¹).

Acknowledgment. Financial support from the Department of Energy—Basic Energy Sciences (DE-FG02-95ER14539) is gratefully acknowledged. V.Yu.B. gratefully acknowledges support from Russia's Foundation for basic research (Grant No. 04-03-32514).

References and Notes

- Mahan, G. D.; Lucas, A. A. *J. Chem. Phys.* **1979**, *68*, 1344.
- Persson, B. N. J.; Ryberg, R. *Phys. Rev. B* **1981**, *24*, 6954.
- Persson, B. N. J.; Liebsch, A. *Surf. Sci.* **1981**, *110*, 356.
- Hammaker, R. M.; Francis, S.; Eischens, R. P. *Spectrochim. Acta* **1965**, *21*, 1295.
- Crossley, A.; King, D. A. *Surf. Sci.* **1977**, *68*, 528.
- Toolenaar, F. J. C. M.; Stoop, F.; Ponc, V. J. *Catal.* **1983**, *82*, 1.
- Stoop, F.; Toolenaar, F. J. C. M.; Ponc, V. J. *Chem. Soc., Chem. Commun.* **1981**, 1024.
- Borovkov, V. Yu.; Luebke, D. R.; Kovalchuk, V. I.; d'Itri, J. L. *J. Phys. Chem. B* **2003**, *107*, 5568.
- Vadlamannati, L. S.; Kovalchuk, V.; d'Itri, J. L. *Stud. Surf. Sci. Catal.* **2000**, *130*, 233.
- Balakrishnan, K.; Schwank, J. J. *Catal.* **1992**, *138*, 491.
- Ponc, V. *Adv. Catal.* **1983**, *32*, 149.
- Shapiro, E. S.; Tkachenko, O. P.; Jaeger, N. I.; Schulz-Ekloff, G.; Grunert, W. *J. Phys. Chem. B* **1998**, *102*, 3798.
- Persson, B. N. J.; Hoffmann, F. M. *J. Electron. Spectrosc. Relat. Phenom.* **1987**, *45*, 215.
- Vadlamannati, L. S.; Kovalchuk, V.; d'Itri, J. L. *Catal. Lett.* **1999**, *58*, 173.
- Zaikovskii, V. I.; Ryndin, Yu. A.; Koval'chuk, V. I.; Plyasova, L. M.; Kuznetsov, B. N.; Yermakov, Yu. I. *Kinet. Catal.* **1981**, *22*, 340.
- Deshmukh, S. S.; Borovkov, V. Yu.; Kovalchuk, V. I.; d'Itri, J. L. *J. Phys. Chem. B* **2000**, *104*, 1277.
- A shoulder at approximately 2120 cm⁻¹ and a low-intensity band at approximately 2170 cm⁻¹ are due to the *P* and *R* branches of the gas-phase CO.
- Sheppard, N.; Nguyen, T. T. *Adv. Infrared Raman Spectrosc.* **1978**, *5*, 67.
- Probably, this band is a singleton of ¹²C¹⁶O linear complexes with electron deficient Pt.
- The increase in the absorbance above approximately 2010–2020 cm⁻¹ in the difference spectra of the adsorbed ¹³C¹⁶O in Figure 4 is an artifact caused by an incomplete compensation of the ¹²C¹⁶O spectrum in the spectrum of the ¹³C¹⁶O + ¹²C¹⁶O mixture.
- The band at 2070 cm⁻¹ was also present when the evacuated catalyst wafer with preadsorbed ¹²C¹⁶O was exposed to ¹³C¹⁶O at equilibrium pressure of 12 Torr (Figure 2).
- Lokhov, Yu. A.; Davydov, A. A. *Kinet. Catal.* **1980**, *21*, 1523.
- Podkolzin, S. G.; Shen, J.; de Pablo, J. J.; Dumesic, J. A. *J. Phys. Chem. B* **2000**, *104*, 4169.
- King, D. A. In *Vibrational Spectroscopy of Adsorbates*; Willis, R. F., Ed.; Springer: Berlin, 1980; p. 179.
- Crossley, A.; King, D. A. *Surf. Sci.* **1980**, *95*, 131.
- Persson, B. N. J.; Tushaus, M.; Bradshaw, A. M. *J. Chem. Phys.* **1990**, *92*, 5034.
- Froitzheim, H.; Hopster, H.; Ibach, H.; Lehwald, S. *Appl. Phys.* **1977**, *13*, 147.
- Adamson, A. W.; Gast, A. P. *Physical Chemistry of Surfaces*; Wiley: New York, 1997.
- Jackson, S. D.; Glanville, B. M.; Willis, J.; McLellan, G. D.; Webb, J.; Moyes, R. B.; Simpson, S.; Wells, P. B.; Whyman, R. J. *Catal.* **1993**, *139*, 207.
- Liu, J.; Xu, M.; Nordmeyer, T.; Zaera, F. J. *Phys. Chem.* **1995**, *99*, 6167.
- Bastein, A. G. T. M.; Toolenaar, F. J. C. M.; Ponc, V. J. *J. Catal.* **1984**, *90*, 88.
- Yeo, Y. Y.; Vattone, I.; King, D. A. *J. Chem. Phys.* **1997**, *106*, 392.
- Lucas, C. A.; Marcović, N. M.; Ross, P. N. *Surf. Sci.* **1999**, *425*, L381.
- Masel, R. I. *Principles of Adsorption and Reaction on Solid Surfaces*; Wiley: New York, 1996, Ch. 3 and references therein.
- Yeo, Y. Y.; Vattuone, L.; King, D. A. *J. Chem. Phys.* **1996**, *104*, 3810.
- Hoffmann, F. M. *Surf. Sci. Rep.* **1983**, *3*, 107.
- Bain, F. T.; Jackson, S. D.; Thomson, S. J.; Webb, G.; Willocks, E. J. *Chem. Soc., Faraday Trans. 1* **1976**, *72*, 2516.
- Heyne, H.; Tompkins, F. C. *Trans. Faraday Soc.* **1967**, *63*, 1274.
- Hollins, P. *Surf. Sci. Rep.* **1992**, *16*, 51.
- Greenler, R. G.; Burch, K. D.; Kretzschmar, K.; Klausner, R.; Bradshaw, A. M. *Surf. Sci.* **1985**, *152/153*, 338.
- Maugé, F.; Binet, C.; Lavalley, J. C. In *Catalysis by Metals*; Renouprez, A. J.; Jobic, H., Eds; Springer-Verlag: Berlin, 1997; Vol. 6, p. 1.
- Yates, J. T. *J. Vac. Sci. Technol. A* **1995**, *13*, 1359.
- Kim, C. S.; Korzeniewski, C. *Anal. Chem.* **1997**, *69*, 2349.
- Solomennikov, A. A.; Lokhov, Y. A.; Davydov, A. A.; Ryndin, Y. A. *Kinet. Catal.* **1979**, *20*, 714.
- Haaland, D. M. *Surf. Sci.* **1987**, *185*, 1.
- Venus, D.; Hensley, D. A.; Kesmodel, L. L. *Surf. Sci.* **1988**, *199*, 391.
- Barth, R.; Pitchai, R.; Anderson, R. L.; Verykios, X. E. *J. Catal.* **1989**, *116*, 61.
- Barth, R.; Ramachandran, A. *J. Catal.* **1990**, *125*, 467.
- Kappers, M. J.; van der Mass, J. H. *Catal. Lett.* **1991**, *10*, 365.
- de Ménorval, L.-C.; Chaquroue, A.; Coq, B.; Figueras, F. J. *Chem. Soc., Faraday Trans.* **1997**, *93*, 3715.
- Mojet, B. L.; Miller, J. T.; Koningsberger, D. C. *J. Phys. Chem. B* **1999**, *103*, 2724.
- Raskó, J. J. *Catal.* **2003**, *217*, 478.
- Bianchi, D. *Curr. Top. Catal.* **2002**, *3*, 161.
- Riguette, B. A.; Damyanova, S.; Gouliev, G.; Marques, C. M. P.; Petrov, L.; Bueno, J. M. C. *J. Phys. Chem. B* **2004**, *108*, 5349.
- Maillard, F.; Savinova, E. R.; Simonov, P. A.; Zaikovskii, V. I.; Stimming, U. *J. Phys. Chem. B* **2004**, *108*, 17893.